INVERSE ANALYSIS OF LARGE-DISPLACEMENT BEAMS

Alejandro E. Albanesi, Victor D. Fachinotti and Alberto Cardona

Centro Internacional de Métodos Computacionales en Ingeniería (CIMEC)
INTEC - Universidad Nacional del Litoral
Guemes 3450, 3000 Santa Fe, Argentina
aalbanes@ceride.gov.ar, ***http://www.cimec.org.ar***

Keywords: Beams, Inverse Analysis, Large-Deflection.

Abstract. The goal of the present work is to introduce a finite element model for the inverse analysis of large-displacements beams in the elastic range. The problem consists in determining the initial shape of the beam such that it attains the design shape under the effect of service loads. This formulation has immediate applications in fields such as compliant mechanism synthesis where flexible links can be modelled as large-deflection beams, among others. The element will be implemented in the MECANO mechanism analysis package and an example to a structural problems is given.

1 INTRODUCTION

The classical (direct) problem in elasticity consists in computing the deformed shape of a body knowing the mechanical properties and the loading in a given undeformed (reference) configuration. We note that this arbitrary deformed configuration is unknown at the start of the analysis and therefore, must be determined as part of the solution process, a process that is inherently non-linear when large deformations are involved. In this work we deal with the inverse problem, that consists in determining the undeformed (reference) configuration, knowing the deformed shape of the body and the loads applied. As described by Fachinotti et al. (2008) this is an inverse design problem, in contrast to classical inverse measurement problems that consist in determining material data knowing both the deformed and undeformed configuration, as well as the service loads.

The formulation described in this paper is the inverse of the well-known, non-linear beam theory, proposed by Cardona and Géradin (1988) to model three-dimensional highly flexible frame structures. These structures necessarily have low mass and very high flexibility, so large displacements behavior ought to be considered. In this theory, flexibility effects are introduced by a hypothesis of large displacements and finite rotations, however, it is assumed that the strains which result are small. The rotational vector is used to parameterize rotations, and these are described as increments with respect to a previous configuration.

Kinematic beam assumptions are formulated before expressing non-linear strain measures and for the purpose of flexible mechanism analysis and synthesis, where intimate beam behavior is not investigated, a simplified beam theory not accounting for high-order strains is adopted, and it is consequently suited for a linear-elastic constitutive relation. We approximate neglecting quadratic pure strain terms, and introduce a linear elastic constitutive relation, which enables us to evaluate the corresponding small-strain axial and moment resultants within the virtual internal work. Finally, it is assumed that beam cross-sections remain straight but can undergo shear strain. It is then clear that under the adopted hypothesis and linear elastic beam stress-strain relations, this model is defined as finite-deformations small-strain.

2 PROBLEM DESCRIPTION

The aim of this section is to describe in detail the model kinematics. In the following, we present the beam in its known *deformed configuration*, and our intention is to obtain the unknown *undeformed configuration*. The kinematic assumptions adopted are the following:

- the beam is initially straight and has uniform cross section,
- beam cross sections remain plane and do not deform during deformation,
- shear deformation of the neutral axis is allowed.

2.1 Beam Kinematics

According to the kinematic assumptions recently made, the given *deformed configuration* of the beam is defined by a right-handed orthonormal frame $\{\mathbf{O}, \mathbf{t}'_1, \mathbf{t}'_2, \mathbf{t}'_3\}$, with $\mathbf{O}$ located on the axis and the family of orthonormal base vectors $\{\mathbf{t}'_1, \mathbf{t}'_2, \mathbf{t}'_3\}$ spanning the planes of cross-sections. Vectors $\mathbf{t}'_1$ and $\mathbf{t}'_2$ are directed along the principal axes of inertia of the rotated cross-section, and $\mathbf{t}'_3$ is its normal vector: $\mathbf{t}'_3 = \mathbf{t}'_1 \times \mathbf{t}'_2$. As the basis $\mathbf{t}'_1, \mathbf{t}'_2, \mathbf{t}'_3\}$ is different at each material point of the line of centroids, it is called the material basis. The beam coordinates under this frame are described by $\{x_1, x_2, x_3\}$, see figure (1). The reference line of centroids is parameterized by the arc-length s' and coincides with the beam coordinate x_3, i.e $s' \equiv x_3$. This
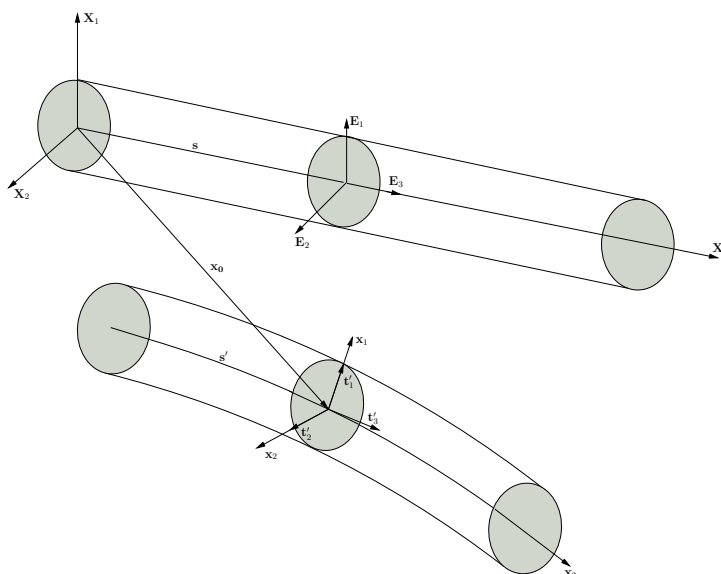
Figure 1: Description of beam kinematics

configuration is described by

$$\mathbf{x} = \mathbf{x_0}(x_3) + x_\alpha \mathbf{t}'_\alpha, \qquad \alpha = 1, 2 \tag{1}$$

where

$$\mathbf{x_0}(x_3) = x_3 \mathbf{t}'_\mathbf{3} \tag{2}$$

represents the position of an axis point and $x_\alpha \mathbf{t}'_\alpha$ is the vector describing the position of a point in the cross section with coordinates x_1 and x_2.

The beam unknown *undeformed configuration* is analogously described by another right-handed orthonormal frame, called *current frame* and defined as $\{\mathbf{o}, \mathbf{E}'_\mathbf{1}, \mathbf{E}'_\mathbf{2}, \mathbf{E}'_\mathbf{3}\}$, with $\mathbf{o}$ located on the undeformed axis and the family of orthonormal base vectors $\{\mathbf{E}'_\mathbf{1}, \mathbf{E}'_\mathbf{2}, \mathbf{E}'_\mathbf{3}\}$ spanning the planes of cross-sections. Vectors $\mathbf{E}'_1$ and $\mathbf{E}'_2$ are directed along the principal axes of inertia of the cross-section, and $\mathbf{E}'_3$ is its normal vector: $\mathbf{E}'_3 = \mathbf{E}'_1 \times \mathbf{E}'_2$. The beam coordinates under this frame are described by $\{X_1, X_2, X_3\}$, see figure (1). The reference line of centroids is parameterized by the arc-length s and coincides with the beam coordinate X_3, i.e $s \equiv x_3$. This undeformed configuration is described by

$$\mathbf{X} = \mathbf{X}_0(x_3) + x_\alpha \mathbf{E}'_\alpha = \mathbf{X}_0(x_3) + \mathbf{Y} \tag{3}$$

where

$$\mathbf{X_0}(x_3) = X_3 \mathbf{E}'_3 \tag{4}$$

represents the position of an axis point and $X_\alpha \mathbf{E}'_\alpha$ is the vector describing the position of a point in the cross section with coordinates X_1 and X_2, and

$$\mathbf{Y} = x_\alpha \mathbf{E}'_\alpha \tag{5}$$

Since the reference frame and the current frame are both orthonormal, we may introduce a rotation tensor $\mathbf{Q}$ and relate the reference and current frame, figure (2), as
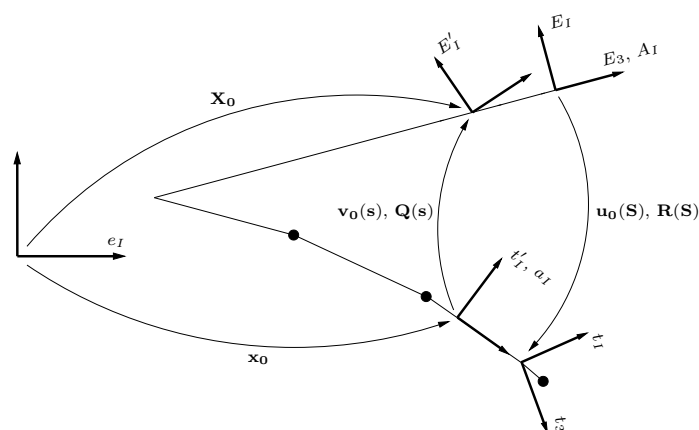
Figure 2: Relation between the reference and current frame

$$\mathbf{E}'_I = \mathbf{Q}(x_3)\mathbf{t}'_I, \qquad I = 1, 2, 3 \tag{6}$$

i.e. we may define the current frame as the rotated reference frame. Then, we rewrite equation (3) as

$$\mathbf{X} = \mathbf{X}_0(x_3) + x_\alpha \mathbf{Q}(x_3)\mathbf{t}'_\alpha \tag{7}$$

and it follows that the cross-section rigidly moves from the reference to the current configuration, and $\mathbf{Q}$ is the *cross-section rigid rotation*. It is interesting to note that, according to equation (6), $\mathbf{Q}$ can be computed as

$$\mathbf{Q}(x_3) = \mathbf{E}'_I \otimes \mathbf{t}'_I \tag{8}$$

and since it is an orthogonal tensor, it can be proven that

$$\mathbf{Q}^T\mathbf{Q} = \mathbf{Q}\mathbf{Q}^T = \mathbf{I} \tag{9}$$

Following the work of Cardona and Géradin (1988), and as mentioned before, a rotation operator is used to describe the cross-section orientation at a given configuration. Starting from the general expression of the rotation operator in terms of the direction $\mathbf{u}$ of the rotation and its amplitude ψ, the parameterization of spherical motion in terms of the Cartesian rotational vector is the most natural one. It has also several advantages, such as the number of parameters which remains minimal, an easy geometric interpretation and the absence of kinematic singularities. The Cartesian rotational vector is defined as the vector which has the direction of the rotation axis $\mathbf{n}$ and a length equal to the amplitude of the rotation ψ

$$\boldsymbol{\psi} = \mathbf{n}\psi \tag{10}$$

In the aforementioned work, which may be referred to as the *beam direct problem*, the rotation operator $\mathbf{R}$ describing the cross-section orientation from the undeformed to the deformed configuration, is defined in terms of the Cartesian rotational vector as

$$\mathbf{R}(\boldsymbol{\psi}) = \mathbf{I} + \frac{\sin\|\boldsymbol{\psi}\|}{\|\boldsymbol{\psi}\|}\widetilde{\boldsymbol{\psi}} + \frac{1 - \cos\|\boldsymbol{\psi}\|}{\|\boldsymbol{\psi}\|^2}\widetilde{\boldsymbol{\psi}}\widetilde{\boldsymbol{\psi}} \tag{11}$$

where the superimposed tilde refers to a $(\mathbf{3x3})$ linear transformation, i.e. $\widetilde{\mathbf{u}}$ associated to a vector $\mathbf{u}$ such as

$$\mathbf{u} = \text{vect}(\widetilde{\mathbf{u}}) \quad \Rightarrow \quad \widetilde{\mathbf{u}} = \begin{bmatrix} 0 & -u_3 & u_2 \\ u_3 & 0 & -u_1 \\ -u_2 & u_1 & 0 \end{bmatrix} \tag{12}$$

and the cross product $\mathbf{u} \times \mathbf{v}$ may be achieved in matrix form premultiplying vector $\mathbf{v}$ by the linear transformation $\widetilde{\mathbf{u}}$

$$\mathbf{u} \times \mathbf{v} = \widetilde{\mathbf{u}}\mathbf{v} \tag{13}$$

The apparent singularity in $\|\boldsymbol{\psi}\| = 0$ which appears in operator $\mathbf{R}$ is easily removed by noticing that

$$\lim_{\|\boldsymbol{\psi}\| \to 0} \mathbf{R}(\boldsymbol{\psi}) = \mathbf{I} \tag{14}$$

2.2 Displacement Gradient Measure of Deformation

In our interest to compute standard three-dimensional deformation measures, we start from the deformation gradient, computing the position gradients with respect to the current parameter s before and after deformation in the material frame, as

$$\mathbf{D}(s, X_1, X_2) = \mathbf{R}^T \frac{d\mathbf{x}}{ds} - \frac{d\mathbf{X}}{ds} \tag{15}$$

Differentiating equations (1) and (3) yields

$$\frac{d\mathbf{X}}{ds} = \mathbf{E_3} \tag{16}$$

and

$$\frac{d\mathbf{x}}{ds} = \frac{d\mathbf{x_0}}{ds} + \frac{d\mathbf{R}}{ds}\mathbf{Y} \tag{17}$$

Expressing equation (17) in the material frame and subtracting equation (16) from it then yields the material measure of deformation

$$\mathbf{D}(s, X_1, X_2) = \mathbf{R}^T \left(\frac{d\mathbf{x_0}}{ds} - \mathbf{e_3} \right) + \mathbf{R}^T \frac{d\mathbf{R}}{ds}\mathbf{Y} \tag{18}$$

It is important to remark that these equations are referenced to the parameter s attached to the unknown, undeformed configuration. Instead, we should reference them to the known parameter s' in the deformed configuration. Using the chain law and differentiating

$$\mathbf{D} = j\,\mathbf{R}^T \left(\frac{d\mathbf{x_0}}{ds'} - \mathbf{e_3} \right) + j\,\mathbf{R}^T \frac{d\mathbf{R}}{ds'}\mathbf{Y} \tag{19}$$

where the Jacobian

$$j = \frac{ds'}{ds} \sim \frac{L}{L_0} \tag{20}$$

is assumed to be the ratio between the length of an element in the deformed configuration L, and its length in the undeformed configuration L_0. Proceeding in an analogous way to that of equation (16), we get

$$\frac{d\mathbf{x_0}}{ds'} = \mathbf{t'_3} \tag{21}$$

The first term in equation (18) may be interpreted as the difference between the axis tangent vector and the normal cross-section vector, and represents the material measure of deformation of the neutral axis

$$\mathbf{\Gamma}(s') = j\,\mathbf{R}^T \mathbf{t'_3} - \mathbf{E_3} \tag{22}$$

The second term of equation (18) involves the rotation of the cross section, and can be interpreted as the material measure of curvature of the neutral axis

$$\widetilde{\mathbf{K}} = j\,\mathbf{R}^T \frac{d\mathbf{R}}{ds'} \tag{23}$$

and represents the rotation gradient along the neutral axis. The components of the corresponding axial vector are found by

$$\mathbf{K} = \mathrm{vect}(\widetilde{\mathbf{K}}) \tag{24}$$

When adopting a parameterization in terms of the Cartesian rotational vector (equation 10), the curvature vector is expressed in the form

$$\mathbf{K} = \mathbf{T}(\boldsymbol{\psi})\frac{d\boldsymbol{\psi}}{ds} \tag{25}$$

where $\mathbf{T}(\boldsymbol{\psi})$ is the so-called tangent operator

$$\mathbf{T}(\boldsymbol{\psi}) = \mathbf{I} + \left(\frac{\cos\|\boldsymbol{\psi}\| - 1}{\|\boldsymbol{\psi}\|^2}\right)\widetilde{\boldsymbol{\psi}} + \left(1 - \frac{\sin\|\boldsymbol{\psi}\|}{\|\boldsymbol{\psi}\|}\right)\frac{\widetilde{\boldsymbol{\psi}}\widetilde{\boldsymbol{\psi}}}{\|\boldsymbol{\psi}\|^2} \tag{26}$$

see Cardona and Géradin (1988). Recalling equation (14), the apparent singularity in $\|\boldsymbol{\psi}\| = 0$ which also appears in the tangent operator is removed by noticing that

$$\lim_{\|\boldsymbol{\psi}\|\to 0} \mathbf{T}(\boldsymbol{\psi}) = \mathbf{I} \tag{27}$$

According to equations (22) and (23), the deformation vector at an arbitrary point of the cross section yields

$$\mathbf{D} = \mathbf{\Gamma} - \widetilde{\mathbf{Y}}\mathbf{K} \tag{28}$$

2.3 Variation of beam strains

In order to develop a virtual work expression of the beam internal deformation, expressions for the variations of the beam strains (equation 22 and 23) are to be computed. For this purpose, we make use of relationships between the variation of the rotation operator and the material and spatial variations of the angular displacements. Let us start from the linear transformation describing spherical motion

$$\mathbf{x} = \mathbf{R}\mathbf{X} \tag{29}$$

The associated virtual displacement is obtained through variation of this expression

$$\delta\mathbf{x} = \delta\mathbf{R}\mathbf{X} \tag{30}$$

and can be recast in one of the forms

$$\delta\mathbf{x} = \delta\mathbf{R}\mathbf{R}^T\mathbf{x} = \delta\widetilde{\boldsymbol{\theta}}\mathbf{x} \qquad \delta\mathbf{x} = \delta\mathbf{R}\left(\mathbf{R}^T\delta\mathbf{R}\right)\mathbf{X} = \mathbf{R}\delta\widetilde{\boldsymbol{\Theta}}\mathbf{X} \tag{31}$$

with the skew-symmetric matrices

$$\delta\widetilde{\boldsymbol{\theta}} = \delta\mathbf{R}\mathbf{R}^T \qquad \delta\widetilde{\boldsymbol{\Theta}} = \mathbf{R}^T\delta\mathbf{R} \tag{32}$$

These matrices represent spatial and material infinitesimal rotations. They are related by

$$\delta\boldsymbol{\Theta} = \mathbf{R}^T\delta\boldsymbol{\theta} \tag{33}$$

The virtual variation of the rotation matrix $\mathbf{R}$ is then obtained from equation (32)

$$\delta\mathbf{R} = \delta\widetilde{\boldsymbol{\theta}}\mathbf{R} = \mathbf{R}\delta\widetilde{\boldsymbol{\Theta}} \tag{34}$$

and its transpose is expressed as

$$\delta\mathbf{R}^T = -\mathbf{R}^T\delta\widetilde{\boldsymbol{\theta}} \tag{35}$$

where $\delta\widetilde{\boldsymbol{\theta}}$ are rotation increments. The variation of the material strain measure equation (22) is computed as follows

$$\delta\boldsymbol{\Gamma} = j\,\delta\mathbf{R}^T\frac{d\mathbf{x_0}}{ds'} + j\,\mathbf{R}^T\frac{d}{ds'}\delta\left(\mathbf{x_0}\right) + \delta j\,\mathbf{R}^T\mathbf{t_3'} \tag{36}$$

$$= j\,\mathbf{R}^T\frac{d}{ds'}\delta\left(\mathbf{x_0}\right) - j\,\delta\widetilde{\boldsymbol{\Theta}}\mathbf{R}^T\frac{d\mathbf{x_0}}{ds'} + \delta j\,\mathbf{R}^T\mathbf{t_3'} \tag{37}$$

while the variation of the material curvature, equation (23), is computed by

$$\delta\widetilde{\mathbf{K}} = j\,\delta\mathbf{R}^T\frac{d\mathbf{R}}{ds'} + j\,\mathbf{R}^T\frac{d}{ds'}\left(\delta\mathbf{R}\right) + \delta j\,\mathbf{R}^T\frac{d\mathbf{R}}{ds'} \tag{38}$$

$$= -j\,\delta\widetilde{\boldsymbol{\Theta}}\widetilde{\mathbf{K}} + j\,\widetilde{\mathbf{K}}\delta\widetilde{\boldsymbol{\Theta}} + \frac{d}{ds'}\left(\delta\widetilde{\boldsymbol{\Theta}}\right) + \delta j\,\delta\widetilde{\boldsymbol{\Theta}} \tag{39}$$

and also

$$= j\,\mathbf{R}^T\frac{d}{ds'}\left(\widetilde{\delta\boldsymbol{\theta}}\right) + \delta j\,\mathbf{R}^T\delta\widetilde{\boldsymbol{\theta}}\mathbf{R} \tag{40}$$

and finally we obtain the expressions of beam strains variations in terms of infinitesimal displacements and rotations

$$\delta\boldsymbol{\Gamma} = j\,\mathbf{R}^T\frac{d}{ds'}\delta\left(\mathbf{x_0}\right) + j\left(\widetilde{\mathbf{R}^T\frac{d\mathbf{x_0}}{ds'}}\right)\delta\boldsymbol{\Theta} + \delta j\,\mathbf{R}^T\mathbf{t_3'} \tag{41}$$

$$\delta\mathbf{K} = j\,\widetilde{\mathbf{K}}\delta\boldsymbol{\Theta} + j\,\frac{d}{ds'}\left(\delta\boldsymbol{\Theta}\right) + \delta j\,\delta\boldsymbol{\Theta} = \mathbf{R}^T\frac{d}{ds'}\left(\delta\boldsymbol{\theta}\right)\frac{L}{L_0} \tag{42}$$

They can be expressed in terms of parameter variations. To this purpose, let us make use of relationships between infinitesimal rotations and parameter variations

$$\delta\boldsymbol{\Theta} = \mathbf{T}(\boldsymbol{\psi})\delta\boldsymbol{\psi} \qquad \frac{d}{ds'}(\delta\boldsymbol{\Theta}) = \mathbf{T}\delta\boldsymbol{\psi}' + \mathbf{T}'\delta\boldsymbol{\psi} \tag{43}$$

We then get

$$\left[\begin{array}{c} \delta\boldsymbol{\Gamma} \\ \delta\mathbf{K} \end{array} \right] = \left[\begin{array}{ccc} \mathbf{R}^T & 0 & \widetilde{\mathbf{R}^T\mathbf{x}_0'} \\ 0 & \mathbf{T} & \widetilde{\mathbf{K}}\mathbf{T} + \mathbf{T}' \end{array} \right] \left[\begin{array}{c} \delta\mathbf{x}_0' \\ \delta\boldsymbol{\psi}' \\ \delta\boldsymbol{\psi} \end{array} \right] \tag{44}$$

2.4 Beam internal work

To establish the equations expressing local equilibrium, let us consider a beam slice between two neighboring cross sections as represented by figure (3), and define the following quantities
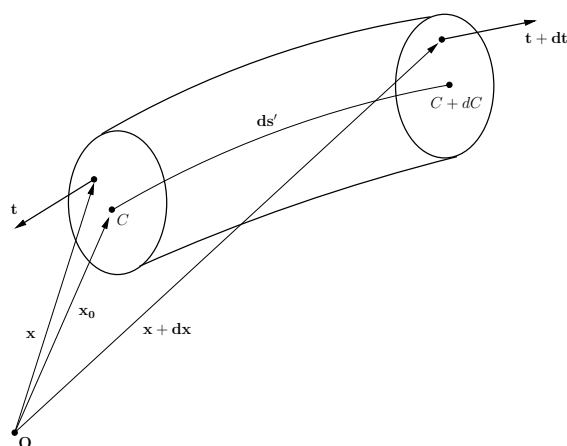

Figure 3: Equilibrium of a beam segment

$$\mathbf{n} = \int_S \mathbf{t} \, dS \tag{45}$$

the *cross section axial/shear force* due to the vector of surface tractions on the cross section $\mathbf{t}$, and

$$\mathbf{m} = \int_S (\widetilde{\mathbf{x} - \mathbf{x}_0})\mathbf{t} \, dS \tag{46}$$

the *moment of surface tractions on the cross section*, due to the vector of surface tractions $\mathbf{t}$ and the distance from the cross-section barycenter $(\mathbf{x} - \mathbf{x}_0)$, then the material counterparts of stress and load resultants are

$$\mathbf{N} = \mathbf{R}^T\mathbf{n} \qquad \mathbf{M} = \mathbf{R}^T\mathbf{m} \tag{47}$$

Following the approach of Géradin and Cardona (2000), we adopt a constitutive law such that the material remains in the linear elastic range, and limit the analysis to the small deformation hypothesis, which consists in assuming that the beam element may undergo large rigid-body

rotations, but that its material strains remain small. Under this assumption, the internal stress resultants are linearly related to the material strains by

$$\left[\begin{array}{c} \mathbf{N} \\ \mathbf{M} \end{array} \right] = \mathbf{C} \left[\begin{array}{c} \boldsymbol{\Gamma} \\ \mathbf{K} \end{array} \right] \tag{48}$$

where $\mathbf{C}$ is the matrix of elastic coefficients. It can be written in more compact form as

$$\boldsymbol{\Sigma} = \mathbf{C}\mathbf{E} \tag{49}$$

with

$$\mathbf{E} = \left[\begin{array}{c} \boldsymbol{\Gamma} \\ \mathbf{K} \end{array} \right] \qquad \boldsymbol{\Sigma} = \left[\begin{array}{c} \mathbf{N} \\ \mathbf{M} \end{array} \right] \tag{50}$$

Under the assumption that the cross section has orthotropic properties, matrix $\mathbf{C}$ takes the form

$$\mathbf{C} = \text{diag}(\begin{array}{cccccc} EA & GA_1 & GA_2 & GI_3 & EI_1 & EI_2 \end{array}) \tag{51}$$

where

EA is the axial stiffness,
GA_1 and GA_2 are the shear bending stiffnesses along the transverse axes,
GI_3 is the torsional stiffness, and
EI_1 and EI_2 are the bending stiffnesses.

The internal virtual work of the beam takes the form

$$\delta\boldsymbol{\pi_{int}} = \int_0^l (\mathbf{N}^T\delta\boldsymbol{\Gamma} + \mathbf{M}^T\delta\mathbf{K})\, ds' = -\int_0^l \delta\mathbf{q}^T\mathbf{B}^T\boldsymbol{\Sigma}\, ds' \tag{52}$$

where $\mathbf{B}$ is the matrix already defined in equation (44)

$$\mathbf{B} = \left[\begin{array}{ccc} \mathbf{R}^T & 0 & \widetilde{\mathbf{R}^T\mathbf{x}_0'} \\ 0 & \mathbf{T} & \widetilde{\mathbf{K}}\mathbf{T} + \mathbf{T}' \end{array} \right] \tag{53}$$

and $\delta\mathbf{q}$ is the 12 degrees of freedom vector

$$\delta\mathbf{q}^T = \left[\begin{array}{cccc} \delta\mathbf{x}_{01}{}^T & \delta\boldsymbol{\psi}_1{}^T & \delta\mathbf{x}_{02}^T & \delta\boldsymbol{\psi}_2{}^T \end{array} \right] \tag{54}$$

Equation (52) can be expressed as

$$\delta\boldsymbol{\pi_{int}} = \delta\mathbf{q}^T\mathbf{F_{int}} \tag{55}$$

with the internal force vector given by

$$\mathbf{F_{int}} = -\int_L \mathbf{B}^T\boldsymbol{\Sigma}\, ds' \tag{56}$$

Finally, the equilibrium of the beam element is obtained in the form

$$\mathbf{R_{es}} = \mathbf{F_{int}} - \mathbf{F_{ext}} \tag{57}$$

and this non-linear equation is solved using the Newton-Raphson method (see Zienkiewicz and Taylor (2000) for details on the implementation of this method in a finite element context).

3   TEST APPLICATION

Let us consider the simple problem of bending a beam in the plane. First, we solve the direct problem, i.e. given the *undeformed* configuration as well as the kinematic boundary conditions and the applied forces, we determine the *deformed* configuration. The beam has length L, the cross section height b is twice the cross section width d, and the load P acts normal to the beam axis. The domain is discreticed using 10 finite elements. The material has isotropic behavior with Young's module E, Poisson ratio ν and shear ratio G. Table 1 and 2 lists the values assumed for material and geometric properties respectively.

Young's module	Poisson ratio	Shear ratio
E = 2.1 $\times 10^5$ N/mm^2	$\nu = 0.25$	G = 8.4 $\times 10^4$ N/mm^2

Table 1: Material data for the beam bending problem.

Beam length	Cross-Section height	Cross-Section width	Load applied
L = 2 $\times 10^3$ mm	b = 60 mm	d = 30 mm	P = 1 $\times 10^5$ N

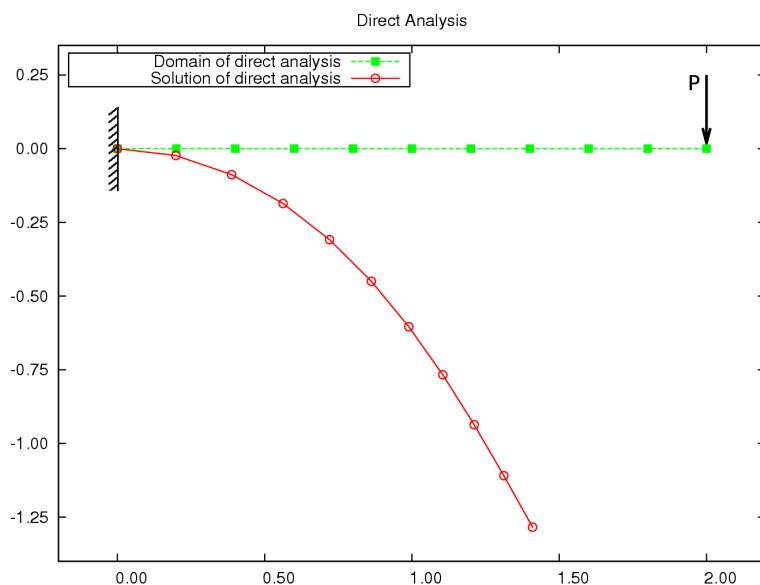Table 2: Model data for the beam bending problem.

Figure 4: Beam direct problem

The domain of the inverse design analysis is the deformed configuration computed as solution of the direct analysis, and its shown in figure (4). The inverse problem is shown in figure (5). The objective of the computation is to verify if we are able to recover the original undeformed configuration as solution.

We define an error measure as the distance between the nodes of the mesh used for the direct analysis, and the positions obtained as solution of the inverse analysis. After solving the equilibrium equation equation (57) with a small residue norm $\|\mathbf{R_{es}}\| < 1 \times 10^{-8}$ (the L_2 norm
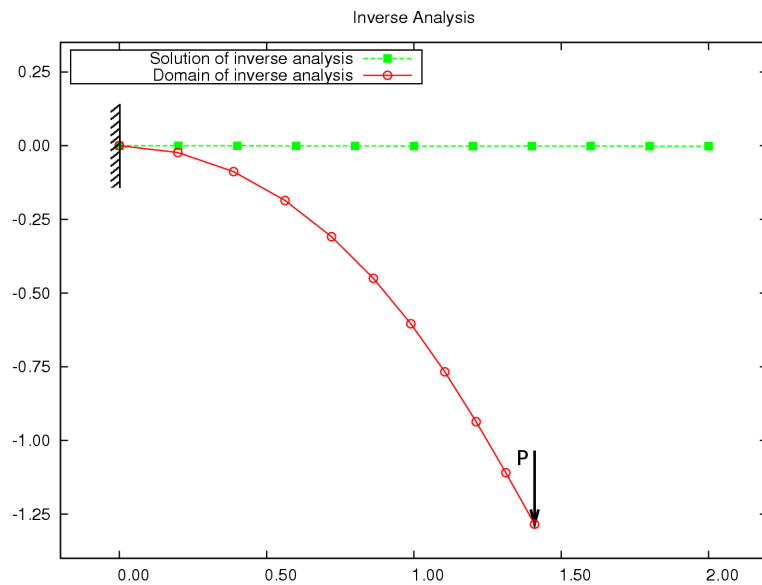
Figure 5: Beam inverse problem

residue vector $\mathbf{R_{es}}$), we obtained a maximum error $\varepsilon < 0.1$ mm at the node where the concentrated force is applied. The relative error with respect to the displacement magnitude is less than 0.015% which demonstrates the outstanding accuracy of the inverse model.

3.1 Validation of the beam bending problem: elliptic integral solution

Elliptic integrals are commonly used to solve large deflection problems in beams under different loading conditions. The most accurate analytical method for predicting very large deflection behavior of flexible beams is the elastica analysis, see for example Bisshopp and Drucker (1945). The resulting integrals that describe the system cannot be solved by usual methods, but they can be manipulated until they are in a form integrable by elliptic integrals. An elliptic integral solution may be used under the assumption that *the beam is linearly elastic, inextensible, rigid in shear and of constant cross section*.
Following an algorithm found in Howell (2001) to solve the elliptic forms described in Byrd and Friedman (1954), we verify the results of our model. The relative error of the elliptic solution with the inverse model is shown in table 3. Once again the errors obtained are very small, and our inverse beam model was successfully verified by a commonly used method in large non-linear deflection of beams.

Horizontal position	Vertical position	Load applied
$\varepsilon_{h_p} = 0.12\,\%$	$\varepsilon_{v_p} = 0.06\,\%$	$\varepsilon_P = 0.3\,\%$

Table 3: Relative error between the elliptic integral solution and the inverse model.

3.2 3D Example

Another important validation test of the model proposed is a 3D example. Let us now consider a structure consisting in an angled beam, loaded out of the structural plane, (figure 6), such that the deformed configuration is bent and twisted in 3D space. Again, we solve the direct problem first, (figure 7), and determine the *deformed* configuration, used as the domain of

the inverse design analysis, (figure 8), to verify if we are able to recover the original undeformed configuration as solution. The material is the same as the previous example, Table 1, and the geometric properties of this model are shown in Table 4.
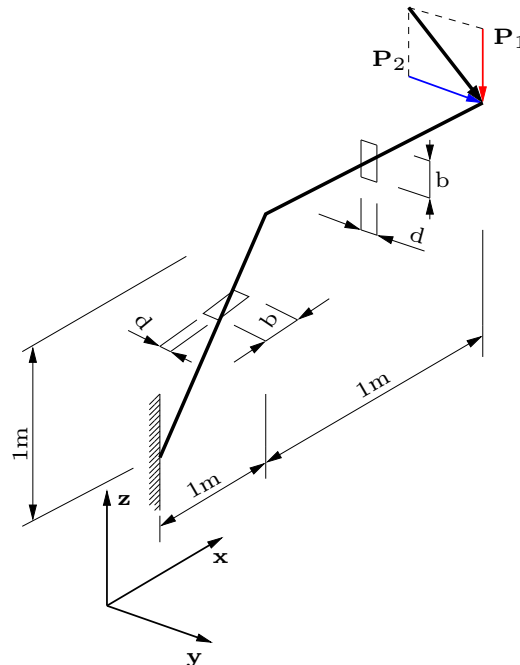

Figure 6: Model of the 3D structure example

Beams length [10^3 mm]	Cross-Section height	Cross-Section width	Loads applied
$L_1 = 1.41$, $L_2 = 1$	b = 100 mm	d = 10 mm	$P_1 = P_2 = 4 \times 10^2$ N

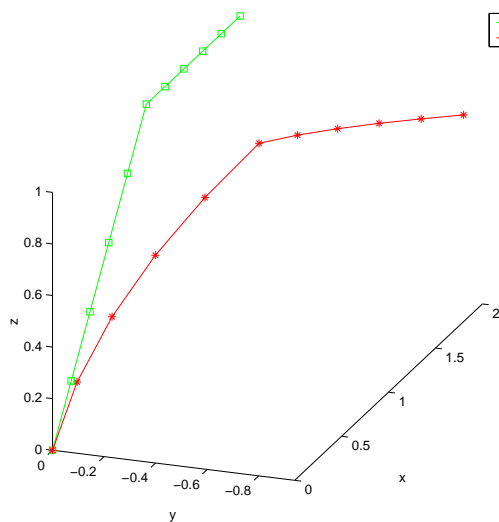Table 4: Geometric properties of the 3D structure example.
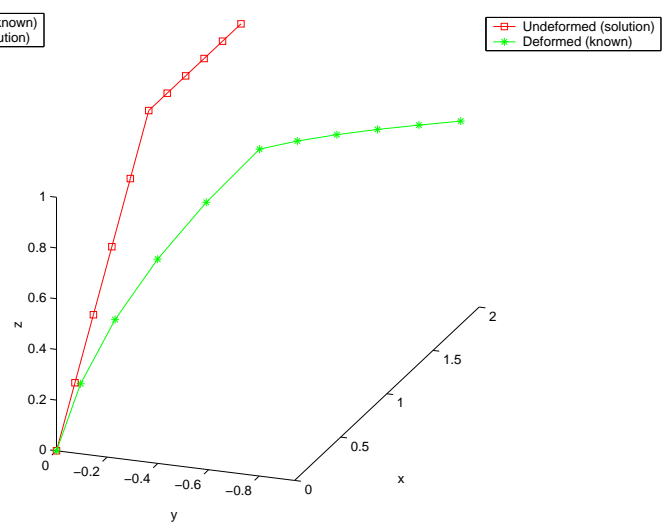

Figure 7: Direct Analysis

Figure 8: Inverse Analysis

Table 5 shows the relative error between the results of the inverse analysis of the 3D structure, and the domain of the direct problem for 10, 20, and 30 elements.

10 elements	20 elements	30 elements
$\varepsilon_{10} = 0.0078$	$\varepsilon_{20} = 0.0076$	$\varepsilon_{30} = 0.0075$

Table 5: Relative error of the model for different number of elements.

4 CONCLUSIONS

The present work introduces a finite element model for inverse analysis of large-displacement beams. It is considered an inverse design problem, where the undeformed configuration is determined knowing the deformed configuration and the loads applied. A linear-elastic constitutive relation is adopted, and the resulting model is defined as finite-deformations small-strain. Planar and 3D examples showed the outstanding accuracy of the model, measured by its ability to recover the original mesh of the corresponding direct analysis. Further, the inverse model was tested and successfully verified using an elliptic integral solution method.

ACKNOWLEDGEMENTS

REFERENCES

K. E. Bisshopp and D. C. Drucker. Large deflections of cantilever beams. *Quarterly of Applied Math*, 3:272–275, 1945.

P. F. Byrd and M. D. Friedman. *Handbook of elliptic integral for engineers and physicists*. Springer-Verlag, Berlin, 1954.

A Cardona and M. Géradin. A beam finite element non-linear theory with finite rotations. *International Journal for Numerical Methods in Engineering*, 26:2403–2438, 1988.

V. Fachinotti, A. Cardona, and P. Jetteur. Finite element modelling of inverse design problems in large deformations anisotropic hyperelasticity. *International Journal for Numerical Methods in Engineering*, 74:894–910, 2008.

M. Géradin and A. Cardona. *Flexible Multibody Dynamics. A Finite Element Approach*. John Wiley & Sons, 2000.

L. L. Howell. *Compliant Mechanisms*. John Wiley & Sons, 2001.

O. C. Zienkiewicz and R. L. Taylor. *The finite element method*, volume 2. Butterworth-Heinemann, London, 2000.